

# Identification of the Substrate Radical Intermediate Derived from Ethanolamine during Catalysis by Ethanolamine Ammonia-Lyase<sup>†</sup>

Güneş Bender,<sup>‡</sup> Russell R. Poyner, and George H. Reed\*

Department of Biochemistry, University of Wisconsin, Madison, Wisconsin 53726

Received July 11, 2008; Revised Manuscript Received August 19, 2008

**ABSTRACT:** Rapid-mix freeze-quench (RMFQ) methods and electron paramagnetic resonance (EPR) spectroscopy have been used to characterize the steady-state radical in the deamination of ethanolamine catalyzed by adenosylcobalamin (AdoCbl)-dependent ethanolamine ammonia-lyase (EAL). EPR spectra of the radical intermediates formed with the substrates, [1-<sup>13</sup>C]ethanolamine, [2-<sup>13</sup>C]ethanolamine, and unlabeled ethanolamine were acquired using RMFQ trapping methods from 10 ms to completion of the reaction. Resolved <sup>13</sup>C hyperfine splitting in EPR spectra of samples prepared with [1-<sup>13</sup>C]ethanolamine and the absence of such splitting in spectra of samples prepared with [2-<sup>13</sup>C]ethanolamine show that the unpaired electron is localized on C1 (the carbinol carbon) of the substrate. The <sup>13</sup>C splitting from C1 persists from 10 ms throughout the time course of substrate turnover, and there was no evidence of a detectable amount of a product like radical having unpaired spin on C2. These results correct an earlier assignment for this radical intermediate [Warncke, K., et al. (1999) *J. Am. Chem. Soc.* 121, 10522–10528]. The EPR signals of the substrate radical intermediate are altered by electron spin coupling to the other paramagnetic species, cob(II)alamin, in the active site. The dipole–dipole and exchange interactions as well as the 1-<sup>13</sup>C hyperfine splitting tensor were analyzed via spectral simulations. The sign of the isotropic exchange interaction indicates a weak ferromagnetic coupling of the two unpaired electrons. A Co<sup>2+</sup>–radical distance of 8.7 Å was obtained from the magnitude of the dipole–dipole interaction. The orientation of the principal axes of the <sup>13</sup>C hyperfine splitting tensor shows that the long axis of the spin-bearing p orbital on C1 of the substrate radical makes an angle of ~98° with the unique axis of the d<sub>z<sup>2</sup></sub> orbital of Co<sup>2+</sup>.

Ethanolamine ammonia-lyase (EAL,<sup>1</sup> EC 4.3.1.7) is an AdoCbl-dependent enzyme that catalyzes elimination of ammonia from the vicinal position of short chain amino alcohols such as ethanolamine to give the corresponding oxo products. The functional protein is believed to be a hexamer of  $\alpha\beta$  dimers [ $(\alpha\beta)_6$ ,  $\alpha$  of ~50 kDa and  $\beta$  of ~31 kDa] (1, 2). EAL is proposed to be an important enzyme in the metabolism of some bacterial species such as *Salmonella enterica*, which can use ethanolamine, derived from the breakdown of phospholipids, as their sole source of carbon, nitrogen, and energy (3). Catalysis by EAL with various substrates and inactivation of EAL with substrate analogues have been studied extensively by kinetic methods, and radical states occurring during catalysis have been probed by EPR spectroscopy (4–9).

The putative catalytic cycle of EAL starts with the formation of a highly reactive 5'-deoxyadenosyl radical and

cob(II)alamin after homolysis of the Co–carbon bond of the cofactor (Scheme 1) (10). The transient 5'-deoxyadenosyl radical abstracts the *pro-S* hydrogen atom from C1 of the substrate to create the initial substrate radical (11). Abstraction of the hydrogen atom from C1 is kinetically coupled to Co–carbon bond homolysis and pulls the Co–carbon bond cleavage process forward (6). The substrate radical rearranges to a product like carbinolamine radical, which abstracts a hydrogen atom from the 5'-carbon of 5'-deoxyadenosine to give a carbinolamine. Breakdown of the carbinolamine to ammonia and acetaldehyde and recombination of the 5'-deoxyadenosyl radical with cob(II)alamin complete the catalytic cycle. Details of the radical rearrangement step are not yet clear. The product radical was proposed to be a carbinolamine radical on the basis of theoretical energy calculations of possible intermediates and transition states (12–14).

EPR spectroscopy reveals the presence of organic radical intermediates spin-coupled to cob(II)alamin whenever reaction mixtures with ethanolamine or with (R)- or (S)-2-aminopropanol are frozen during turnover (15–18). EPR spectra of the paramagnetic species consist of the  $g_x$  and  $g_y$  signals of cob(II)alamin at  $g \sim 2.2$ ,  $g_z$  at  $g \sim 1.98$ , and the signal of the organic radicals at  $g \sim 2.003$  (17). Cob(I)-alamin and the organic radicals interact magnetically through exchange and dipole–dipole interactions, creating spectra in which signals for each paramagnetic species are

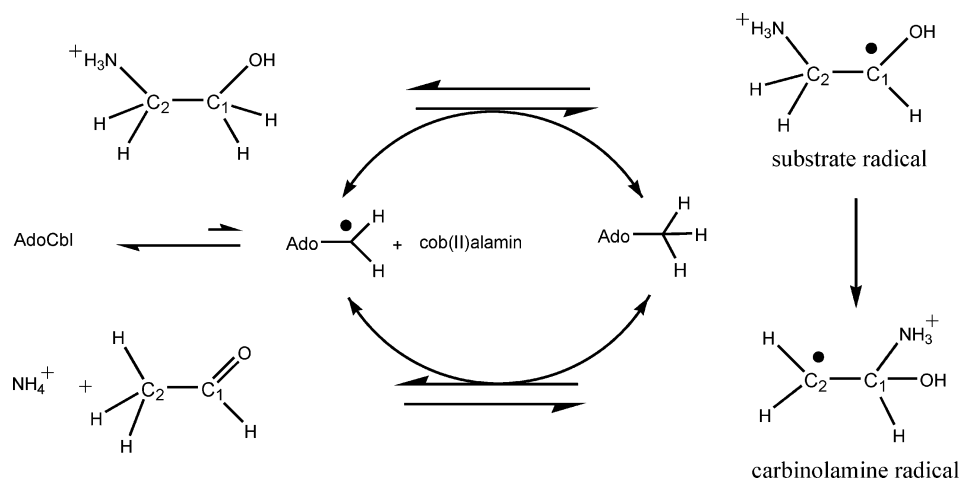
<sup>†</sup> This research was supported by NIH Grant R56-GM35752.

\* To whom correspondence should be addressed: University of Wisconsin, 1710 University Ave., Madison, WI 53726-4087. Telephone: (608) 262-0509. Fax: (608) 265-2904. E-mail: ghreed@wisc.edu.

<sup>‡</sup> Present address: University of Michigan Medical School, 1150 W. Medical Center Dr., MSRB III, Ann Arbor, MI 48109-0606.

<sup>1</sup> Abbreviations: EAL, ethanolamine ammonia-lyase; AdoCbl, 5'-deoxyadenosylcobalamin; EPR, electron paramagnetic resonance; NMR, nuclear magnetic resonance; RMFQ, rapid-mix freeze-quench; HEPES, N-(2-hydroxyethyl)piperazine-N'-2-ethanesulfonic acid; KIE, kinetic isotope effect; IE, isotope effect.

Scheme 1



perturbed by the electron–electron spin coupling with the partner (19).

The EPR spectrum of a radical intermediate in the reaction of EAL with ethanolamine was previously assigned as a productlike carbinolamine having unpaired spin on C2 (20). The distance between the radical intermediate and the cobalt center of cob(II)alamin was determined to be  $\sim 9.7$  Å (21). Theoretical hyperfine splitting values of different possible radical identities and conformations were obtained using electronic structure calculations (22). The structure of a radical intermediate of ethanolamine was further characterized by electron spin echo envelope modulation spectroscopy (13, 23, 24). However, conclusions from all of these studies were based on the original assignment of the radical intermediate as the carbinolamine product radical (20). In the earlier studies, concentrated solutions of enzyme were premixed with a concentrated solution of ethanolamine (20). The reaction was initiated by addition of AdoCbl to the enzyme/substrate mixture prior to manual freezing of the reaction mixtures. There is a slow binding of AdoCbl to the enzyme that delays consumption of substrate using this order of addition (25, 26). AdoCbl binds to the enzyme with high affinity, and its binding and dissociation are probably not part of the normal catalytic cycle (27). Moreover, significant amounts of acetaldehyde and ammonia are generated during the several seconds required to mix and freeze the sample.

In this study, the radical intermediate observed during the steady-state regime in the reaction of EAL with ethanolamine is characterized by RMFQ trapping methods (28). These methods make it possible to use much lower concentrations of substrate and buffer and to use the physiological order of addition of substrate to the enzyme–cofactor complex. The radical intermediates are probed throughout the time course of substrate turnover with C1 and C2 isotopomers of ( $^{13}\text{C}$ )ethanolamine. Distance and geometrical information regarding the positions of the radical relative to cob(II)alamin is obtained from detailed analysis of electron spin–spin and nuclear spin–electron spin interactions.

## EXPERIMENTAL PROCEDURES

**Materials.** AdoCbl was purchased from Sigma-Aldrich. [1- $^{13}\text{C}$ ]Ethanolamine was purchased from Cambridge Isotopes, and [2- $^{13}\text{C}$ ]ethanolamine was purchased from Isotec. The position of  $^{13}\text{C}$  in commercial samples of ( $^{13}\text{C}$ )ethano-

lamine was confirmed by  $^{13}\text{C}$  NMR (see the Supporting Information). The  $^{13}\text{C}$  chemical shift of C1 is more downfield ( $\sim 61$  ppm) than the  $^{13}\text{C}$  chemical shift of C2 ( $\sim 45$  ppm). The chemical shifts of the commercial samples of ( $^{13}\text{C}$ )ethanolamine were further compared to the chemical shifts of samples of ( $^{13}\text{C}$ )ethanolamine synthesized from ( $^{13}\text{C}$ )glycine. The labeling patterns of the synthetic samples were verified by the one-bond or two-bond  $^1\text{H}$ – $^{13}\text{C}$  coupling constants of the starting materials, [2- $^{13}\text{C}$ ]glycine and [1- $^{13}\text{C}$ ]glycine.

**Purification of EAL.** EAL of *Salmonella typhimurium* (EC 4.3.1.7) was overexpressed in *Escherichia coli* and purified as previously described (4). All steps of purification were conducted at 4 °C. After ammonium sulfate precipitation, the enzyme was solubilized via dialysis against 10 mM HEPES/NaOH (pH 7.5) for  $\sim 48$  h, with five or six buffer changes. At the end of dialysis, the insoluble material was removed by centrifugation at 30000g for 30 min. The final enzyme concentration was 40–50 mg/mL, and the specific activity was  $\sim 30$ – $45$   $\mu\text{mol}$  of ethanolamine per minute per milligram of EAL at 25 °C, as determined by the EAL–alcohol dehydrogenase coupled assay (27). Concentrations of apo-EAL were measured spectrophotometrically at 280 nm using an extinction coefficient of  $0.69 \text{ mL mg}^{-1} \text{ cm}^{-1}$ , a molecular mass of 82 kDa of an  $\alpha\beta$  unit of the  $(\alpha\beta)_6$  protomer, and six active sites per protomer (4).

**Stopped Flow Spectrophotometry.** The extent of Co–carbon bond cleavage in AdoCbl during the steady state of the reaction of EAL with ethanolamine was assayed by stopped flow spectrophotometry. The measurements were carried out with an Applied Photophysics SX.18MV-R reaction analyzer. The transient decrease in absorption of AdoCbl at 525 nm was monitored upon mixing of a solution of the EAL–AdoCbl complex with ethanolamine. Calibration of Co–carbon bond cleavage was accomplished by mixing the EAL–AdoCbl complex with an excess of hydroxyethylhydrazine. The latter suicide inhibitor effects a stoichiometric conversion of enzyme-bound AdoCbl to its cleaved form, cob(II)alamin (4).

**Preparation of Samples by RMFQ and Acquisition of EPR Spectra.** RMFQ samples were prepared using an Update Instruments RAM syringe essentially in the same manner that was described previously (28, 29). EAL and AdoCbl, both in 10 mM HEPES/NaOH (pH 7.5), were premixed at 0.46 mM enzyme (active sites) and 0.62 mM AdoCbl to form

the holoenzyme. The holoenzyme solution was mixed with 8 mM ethanolamine (pH 7.5) using the rapid mixing apparatus. The reactions were freeze-quenched when the mixtures were injected into cold isopentane ( $-130^{\circ}\text{C}$ ). Following packing at  $-130^{\circ}\text{C}$ , the samples were stored in liquid  $\text{N}_2$ . X-Band EPR spectra were recorded at 77 K using a Varian E-3 EPR spectrometer and a standard liquid  $\text{N}_2$  immersion Dewar. Data were acquired digitally through a custom interface and a personal computer using modified XEMR (version 0.7) software.

**Spectral Simulations.** Magnetic interaction parameters were obtained through simulation of EPR spectra using the following spin Hamiltonian (4):

$$H = \beta B \cdot g_1 \cdot S_1 + \beta B \cdot g_2 \cdot S_2 + JS_1 \cdot S_2 + S_1 \cdot D \cdot S_2 + H_{\text{HFI}} \quad (1)$$

The first two terms in eq 1 present the electronic Zeeman interaction of low-spin  $\text{Co}^{2+}$  ( $S_1$ ) and the organic radical ( $S_2$ ). The third and fourth terms describe the exchange ( $J$ ) and the dipole–dipole ( $D$ ) interactions between the two electron spins, respectively. The final term describes the hyperfine interactions ( $H_{\text{HFI}}$ ) between the electron spins and nuclear spins. Orthogonal transformations, using Euler angles, are used to express the tensor quantities in eq 1 in a common reference frame that was chosen to be the  $g$  axis system of the low-spin  $\text{Co}^{2+}$ . The Euler rotations used the “x-convention” as described by Goldstein (30). Additional details of the diagonalization of the energy matrix and generation of “field-swept” EPR spectra are provided in previous papers (4, 31). The fitting was done by trial and error.

In the EPR spectra, the  $\text{Co}^{2+}$  radical pair, hyperfine splittings from  $^{59}\text{Co}$  ( $I = 7/2$ ) of cob(II)alamin and from  $1\text{-}^{13}\text{C}$  ( $I = 1/2$ ) in the sample of labeled ethanolamine are the only resolved hyperfine features in the spectra. Hyperfine splittings from  $^{14}\text{N}$  ( $I = 1$ ) of the dimethylbenzimidazole lower axial ligand of  $\text{Co}^{2+}$  (29, 32, 33) and from  $\alpha\text{-}^1\text{H}$  ( $I = 1/2$ ),  $\beta\text{-}^{14}\text{N}$  ( $I = 1$ ), and two  $\beta\text{-}^1\text{H}$  atoms are not resolved and contribute an inhomogeneous broadening in the signals. Estimates of hyperfine splitting parameters of these latter nuclear spins were derived from separate studies of selectively deuterated,  $^{13}\text{C}$ , and  $^{15}\text{N}$  isotopologues of ethanolamine (34). These parameters were included in these simulations to account for the inhomogeneous line widths.

## RESULTS

**Extent of Cobalt–Carbon Bond Cleavage in the Steady State.** Cleavage of the Co–carbon bond of AdoCbl results in a decrease in the absorbance at 525 nm. The transient drop in absorbance upon mixing solutions of the EAL–AdoCbl complex with ethanolamine was compared to the absorbance change observed upon stoichiometric cleavage of enzyme-bound AdoCbl with hydroxyethylhydrazine (4). The transient  $\Delta A_{525}$  for the reaction with ethanolamine is approximately  $70 \pm 5\%$  of the 100% cleavage achieved with hydroxyethylhydrazine (Figure S2 of the Supporting Information).

**Observation of the Earliest Paramagnetic Intermediate.** EPR spectra of samples corresponding to 10 ms following mixing of substrate with the enzyme–cofactor complex exhibit signals at  $g$  values corresponding to low-spin  $\text{Co}^{2+}$  and organic free radical, respectively (see spectrum a of Figure 1A). Signals for both the low-spin  $\text{Co}^{2+}$  and organic free radical are perturbed by the electron spin–spin coupling

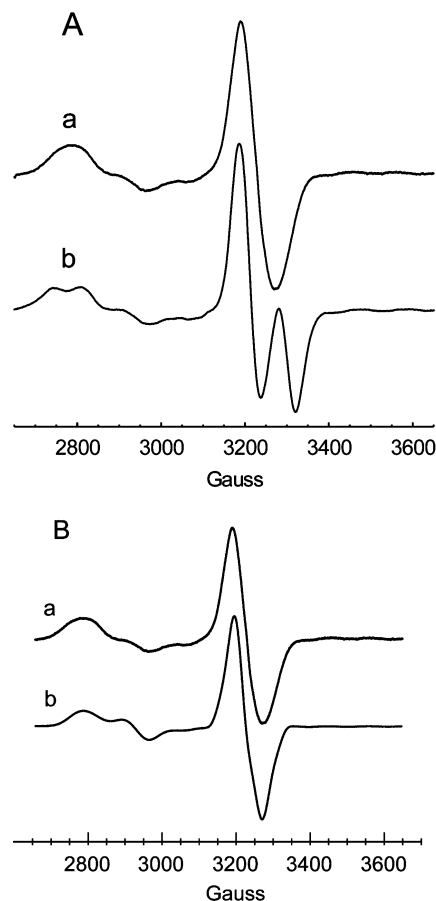


FIGURE 1: (A) Comparison of the EPR spectra of the steady-state radical intermediates obtained with (a) ethanolamine by RMFQ at 10 ms and (b) (*S*)-2-aminopropanol obtained by mixing and manually freezing the sample. For ethanolamine (a), the solution of EAL (0.46 mM active sites) and AdoCbl (0.62 mM) in 10 mM Hepes/NaOH (pH 7.5) was mixed with an equal volume of 8 mM ethanolamine in 10 mM Hepes/NaOH adjusted to pH 7.5. For the sample of (*S*)-2-aminopropanol (b), the sample contained initially 0.2 mM EAL (active sites), 0.4 mM AdoCbl, and 2 mM (*S*)-2-aminopropanol in 10 mM Hepes/NaOH adjusted to pH 7.5. (*S*)-2-Aminopropanol was added last, and the sample was frozen in  $\sim 20$  s by dipping the EPR tube into a chilled slush of isopentane. The spectra were recorded at 77 K. Spectrum a is the average of eight 240 s scans, and spectrum b is the average of four 240 s scans. Spectra were recorded at 9.05 GHz (“free electron”,  $g = 2.0023$  at 3230 G) under a nonsaturating microwave power (4 mW) and a field modulation of 8 G. (B) Comparison of experimental (a) and simulated (b) EPR spectra of the steady-state radical obtained with ethanolamine as the substrate. The experimental conditions are those described for panel A. The following parameters were used in the simulation:  $J = -53$  G;  $D = -43$  G;  $E = -4$  G; Euler angles for the **D** tensor of  $0^\circ$ ,  $25^\circ$ , and  $0^\circ$ ; **g** tensor of  $\text{Co}^{2+}$  of [2.232, 2.205, 1.975]; **A** tensor of  $^{59}\text{Co}$  of [7G, 4G, 109G]; line width of  $\text{Co}^{2+}$  transitions of 25 G (isotropic);  $A_{\text{iso}}^{14}\text{N}$  lower axial ligand at 15 G; substrate radical **g** tensor of [2.005, 2.003, 2.002]; **A** tensor of the  $\alpha$ -proton of [ $-35$  G,  $-22$  G,  $-4$  G]; Euler angles of  $140^\circ$ ,  $-110^\circ$ , and  $-130^\circ$ ;  $A_{\text{iso}}$  of  $\beta\text{-H}_a$  of 12.5 G;  $A_{\text{iso}}$  of  $\beta\text{-H}_b$  of 5.5 G;  $A_{\text{iso}}$  of  $^{14}\text{N}$  (ethanolamine) of 12 G; line width of radical transitions of 12 G (isotropic). As noted in the text, the hyperfine splitting parameters representing unresolved hyperfine structure were included in the simulation to account for the inhomogeneously broadened lines. These parameters were derived from separate simulations of spectra of selectively deuterated samples in  $\text{D}_2\text{O}$  (34).

interactions. In contrast to the “radical doublet” (see spectrum b of Figure 1A) observed in analogous spectra of the intermediate observed with the 2-aminopropanols (17, 18, 29), the EPR signal of the organic radical component produced with ethanolamine gives a broad singlet.

The appearance of the radical component in the  $\text{Co}^{2+}$ –radical spin-coupled pair depends on the relative signs of the exchange coupling parameter,  $J$ , and the dipole–dipole coupling parameter,  $D$  (see eq 1) (29). The latter parameter is negative, by convention (35). Splittings from the effects of exchange and of dipole–dipole coupling add constructively in the central region of the radical spectrum whenever  $J$  and  $D$  are opposite in sign, and that situation occurs when the exchange coupling is antiferromagnetic (see spectrum b of Figure 1A) (29). On the other hand, for the case of ferromagnetic coupling (i.e.,  $J$  negative using the sign convention in eq 1), splitting from the exchange and from the dipole–dipole interactions will tend to offset one another in the middle of the pattern (29). Simulations of these spectra (Figure 1B) as well as those obtained from samples made with perdeuterated ethanolamine indicate that the exchange interaction is ferromagnetic (34). The switch from a doublet signal to a broad singlet upon going from the slow substrates, (*S*)- and (*R*)-2-aminopropanol, to ethanolamine can therefore be attributed to a change in the sign of the exchange coupling parameter,  $J$ , instead of a dramatic change in the interspin distance. Except for the sign of  $J$ , the magnitudes of the electron spin coupling parameters ( $J = -53 \pm 2$  G and  $D = -43 \pm 5$  G) are in the same range as those found for the substrate radical of (*S*)-2-aminopropanol ( $J = 70$  G and  $D = -23$  G) (29). Euler angles relating the  $\mathbf{D}$  tensor to the  $g$  axis system of  $\text{Co}^{2+}$  are  $0^\circ$ ,  $25 \pm 10^\circ$ , and  $0^\circ$ . The interspin vector and the  $z$ -axis of  $\text{Co}^{2+}$  therefore describe an angle of  $\sim 25^\circ$ . The small  $E$  term ( $-4$  G) may result from the slight off-axis positioning of the two spins (36).  $|J|$  is close to that reported recently; however, Sun et al. (37) and Canfield and Warncke (24) use a model of antiferromagnetic coupling. It is also noteworthy that in the EPR spectra reported by Sun et al. (37), the radical signal obtained with unlabeled ethanolamine is split into a doublet, unlike the singlet spectrum reported here for the RMFQ sample with unlabeled ethanolamine. It is possible to generate splitting (data not shown) by combinations of high salt and glycerol used in the buffer system of Sun et al. (37). However, under these same conditions, there is a noticeable amount of precipitation of the protein isolated by the procedure of Bandarian and Reed (4). This latter procedure avoids the use of Triton that was part of the purification originally described by Faust and Babior (2) and used by Sun et al. (37). Changes in the character of the EPR spectra with different buffer or salt conditions indicate that these solution components alter the active site in a manner that influences the spin–spin coupling parameters. The activity of the enzyme is, however, virtually the same in the buffer used here and in that used by Sun et al. (37).

Adjustments to  $J$  and  $D$  allow simulation of the broad singlet spectrum for the radical observed with ethanolamine using an antiferromagnetic coupling scenario. However, when deuterated substrates and  $\text{D}_2\text{O}$  are used, the improved resolution in the spectrum, wherein additional hyperfine structure is visible, makes it impossible to simulate the spectra with antiferromagnetic coupling (34).

**Location of Unpaired Spin in the Radical Intermediate.** Spectra obtained at 10 ms for samples of unlabeled ethanolamine,  $[2\text{-}^{13}\text{C}]$ ethanolamine, and  $[1\text{-}^{13}\text{C}]$ ethanolamine are compared in Figure 2. Clearly, the radical appearing at 10 ms has unpaired spin at C1 where it couples strongly to the

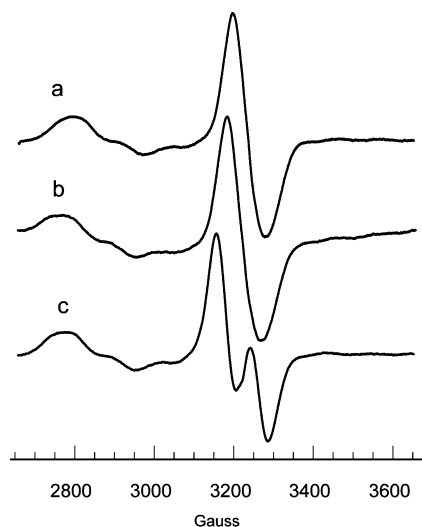


FIGURE 2: EPR spectra of RMFQ samples with unlabeled ethanolamine and with isotopomers of  $(^{13}\text{C})$ ethanolamine. The sample compositions are given in the legend of Figure 1 except for substitution of (b)  $[2\text{-}^{13}\text{C}]$ ethanolamine and (c)  $[1\text{-}^{13}\text{C}]$ ethanolamine for (a) ethanolamine. The reactions were freeze-quenched at 10 ms. Each spectrum represents the average of six scans. Other acquisition parameters were like those in the legend of Figure 1.

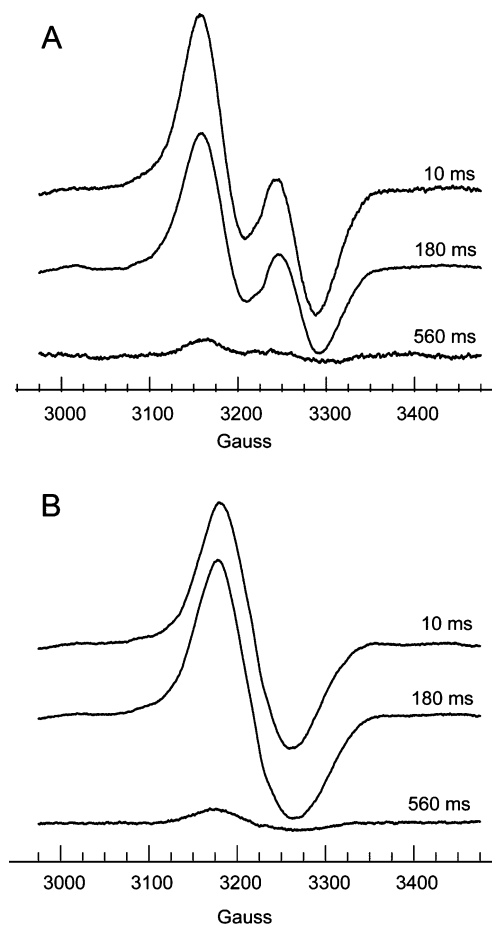


FIGURE 3: Time course of the EPR signal of the radical intermediate with either (A)  $[1\text{-}^{13}\text{C}]$ ethanolamine or (B)  $[2\text{-}^{13}\text{C}]$ ethanolamine as the substrate. The respective reaction times when the reactions were freeze-quenched are given. Acquisition parameters were like those in the legend of Figure 1.

$^{13}\text{C}$  nuclear spin. The time courses for the reactions with the isotopomers of  $(^{13}\text{C})$ ethanolamine (Figure 3) show that the hyperfine splitting from  $[1\text{-}^{13}\text{C}]$ ethanolamine persists



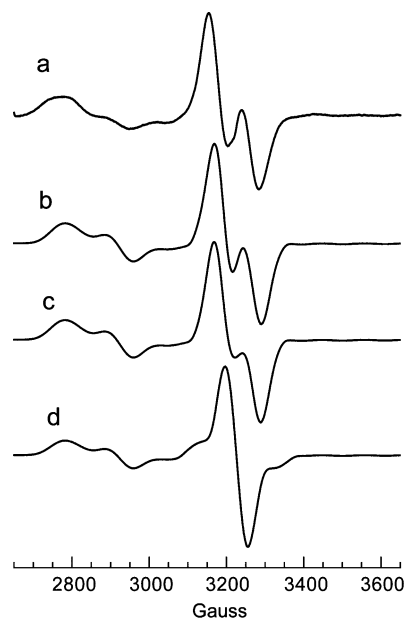


FIGURE 4: Analysis of the  $^{13}\text{C}$  hyperfine splitting interaction in EPR spectra of the substrate radical during the reaction of  $[1-^{13}\text{C}]$ ethanolamine. (a) Experimental spectrum taken at 10 ms. (b) Spectrum calculated using a  $^{13}\text{C}$  hyperfine tensor of [10 G, 10 G, 120 G] and Euler angles of  $0^\circ$ ,  $98^\circ$ , and  $20^\circ$ . (c) Spectrum calculated using a  $^{13}\text{C}$  hyperfine tensor of [7 G, 13 G, 110 G] and Euler angles of  $0^\circ$ ,  $98^\circ$ , and  $20^\circ$ . (d) Spectrum calculated using the same  $^{13}\text{C}$  tensor as in part c but with Euler angles of  $0^\circ$ ,  $0^\circ$ , and  $0^\circ$ . The other simulation parameters are like those in the legend of Figure 1.

throughout the course of substrate turnover, whereas no hyperfine splitting appears for  $^{13}\text{C}$  at C2. These observations indicate that the substrate radical is the dominant paramagnetic species arising from the substrate during the entire time course of the reaction. Differences in the line shape of the spectrum of the radical with different buffer and salt compositions (noted above) do not, however, account for the position of  $^{13}\text{C}$  sensitivity, which is at C1 using either the present RMFQ protocol or the buffer system and manual mixing and freezing protocol of Warncke et al. (20). Radical intermediates that occur after rearrangement of the substrate radical do not reach concentrations sufficient to allow detection by EPR. The results reported in Figures 2 and 3 have led to a correction of the original assignment of the radical signals to a rearranged or product radical species (38).

**Analysis of the  $^{13}\text{C}$  Hyperfine Interaction.** Central atom hyperfine splitting interactions in  $\pi$  radicals are typically strong, anisotropic, and approximately axially symmetric (39, 40). A  $^{13}\text{C}$  hyperfine interaction tensor was introduced into the spectral simulations to characterize this electron spin–nuclear spin interaction. Inclusion of the  $^{13}\text{C}$  hyperfine interaction in spectral simulations requires that the  $^{13}\text{C}$  hyperfine splitting tensor (together with the other tensors in eq 1) be expressed in a common frame of reference, which is taken to be the  $g$  axis system of the low-spin  $\text{Co}^{2+}$ . Results of the simulations are compared to the experimental spectrum in Figure 4.  $^{13}\text{C}$  hyperfine tensors ranging from [7, 13, 110] to [12, 12, 120] (values in gauss) reproduce the observed splitting in the experimental spectra. Euler angles relating the  $^{13}\text{C}$  hyperfine tensor to the  $g$  axis were  $0^\circ$ ,  $98 \pm 2^\circ$ , and  $20 \pm 10^\circ$ . The simulations demonstrate that the line shape is particularly sensitive to the orientation (second Euler angle) of the  $z$  axis of the  $^{13}\text{C}$  hyperfine tensor with respect to the  $g_z$  axis of  $\text{Co}^{2+}$ , and this second Euler angle shows that the

unique axis of the spin-bearing  $p$  orbital of the substrate radical is oriented approximately perpendicular to the unique axis of the  $d_{z^2}$  orbital of  $\text{Co}^{2+}$ . The approximately axial symmetry of both tensors renders the direction of  $A_z$   $^{13}\text{C}$  relative to  $g_x$  and  $g_y$  of  $\text{Co}^{2+}$  essentially arbitrary.

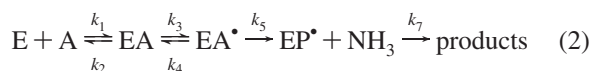
## DISCUSSION

**Mechanistic Significance of the Substrate Radical.** Optical spectra obtained by stopped flow, in which the enzyme–AdoCbl complex is mixed with ethanolamine, indicate that  $\sim 70\%$  of the enzyme-bound AdoCbl is cleaved to cob(II)-alamin in the steady state of the reaction. These EPR results indicate that virtually all of this cleaved cofactor is in a complex with the substrate radical of ethanolamine because the EPR spectra do not show detectable amounts of other radicals. This result in turn suggests that cleavage of the C–N bond in the substrate radical is a significant barrier in the overall reaction. This conclusion is in accord with the observation of a  $^{15}\text{V}/\text{K}$  KIE that was reported earlier from isotope ratio mass spectrometric measurements (18). The observation of a  $^{15}\text{V}/\text{K}$  KIE shows that the reaction is reversible in all steps up to and including the formation of the substrate radical. These steps include Co–carbon bond cleavage and abstraction of the *pro-S* hydrogen atom from C1 of ethanolamine. The fact that the  $^{15}\text{V}/\text{K}$  KIE (1.0017) is significantly smaller than that expected from full expression of a nitrogen IE (1.03) suggests that the forward commitment is high. The  $^{15}\text{N}$  KIE may be more fully expressed in  $V_{\text{max}}$ . Preliminary results show that the  $^{15}\text{V}$  obtained by direct comparison is significantly larger than the measured  $^{15}\text{V}/\text{K}$  KIE (R. R. Poyner, M. A. Anderson, W. W. Cleland, and G. H. Reed, preliminary results).

The assignment of the substrate radical in the steady state also brings ethanolamine into register with results for (*S*)-2-aminopropanol, where the substrate radical is present in the steady state (17, 29). The reports (13, 20, 23) of a rearranged substrate (carbinolamine) radical were surprising from the viewpoint of the predicted stability of free radicals. In addition to the intrinsic lability of hemiaminals, the carbinolamine radical would have hyperconjugation of  $\beta$  substituents as its sole means of spin delocalization. On the other hand, several resonance structures are possible for the substrate radical in which the radical center is adjacent to an OH group (41). The fact that radical intermediates following cleavage of the C–N bond of the substrate radical are too unstable, and thereby too dilute, for detection by EPR spectroscopy means that the rearrangement step of the catalytic cycle remains elusive in contrast to the earlier suggestions (13). The assignment of the radical center to C1 of ethanolamine also obviates the need to invoke two conformations of the radical to account for the duality of  $\beta$ -proton couplings seen in electron spin echo envelope modulations (24) because the substrate radical has two distinct  $\beta$ -protons.

Assignment of the substrate radical as the predominant intermediate in the reaction of EAL with ethanolamine simplifies interpretations of  $V$  and of  $V/\text{K}$  KIEs. If steps subsequent to the rearrangement were to be significantly rate-limiting, then any paramagnetic species associated with these intermediates should be detectable in the steady state. Thus, it is now clear that the  $^{15}\text{N}$  sensitive step assayed as

$^{15}(V/K)$  in the isotope ratio mass spectrometry measurements is the initial cleavage of the C2–N bond of the substrate radical (17). The steady-state mechanism fits the model shown in eq 2:



where EA is the enzyme–ethanolamine complex, EA\* is the complex with the substrate radical, EP\* is a product radical complex, and the  $k_7$  arrow includes all of the remaining steps leading to products. Although step  $k_5$  is written as leading to a product radical, EP\*, and ammonia, there is, at present, no evidence against an intramolecular rearrangement without release of free ammonia. It is clear, however, that step  $k_5$  involves cleavage of the C2–N bond. Because the concentrations of intermediates following C2–N bond cleavage are too low to be detected, the step represented by  $k_5$  is effectively the first irreversible step, and  $V/(KE_T)$  becomes

$$\frac{V}{KE_T} = \frac{k_1 k_3 k_5}{k_2 k_5 + k_2 k_4 + k_3 k_5} \quad (3)$$

The expression for  $V/E_T$  is

$$\frac{V}{E_T} = \frac{k_3 k_5 k_7}{k_3 k_7 + k_4 k_7 + k_5 k_7 + k_3 k_5} \quad (4)$$

These equations can be used to derive expressions for the KIEs on  $V$  and on  $V/K$  in terms of the intrinsic rate constants (42, 43).

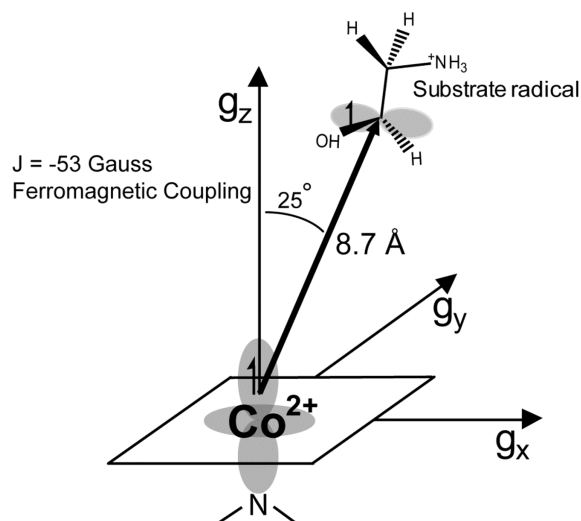
**Structural Conclusions from the Spin–Spin Interaction Parameters.** The magnitude and sign of the exchange interaction ( $J = -0.005 \text{ cm}^{-1}$ ) reflect a weak ferromagnetic exchange interaction between the unpaired electron on the radical and the unpaired electron in the  $d_z^2$  orbital of  $\text{Co}^{2+}$ . Because such weak interactions are likely mediated by spin polarization in intervening matter (superexchange) and the nature of intervening matter is not known, neither the magnitude nor the sign of  $J$  can be readily interpreted in structural terms (35). However, as noted above, both the sign and magnitude of  $J$  have a significant influence on the appearance of the spectra. The approximately  $98^\circ$  angle between the respective unique axes of the two spin-bearing orbitals versus an approximately colinear orientation in the corresponding situation with the substrate radical of (*S*)-2-aminopropanol (29) is almost certainly a factor in the differences in the signs and magnitudes of the exchange interactions observed for these two substrates (35). These differences in orbital alignment and distances between the radical centers and  $\text{Co}^{2+}$  observed with the substrate radicals of (*S*)-2-aminopropanol and ethanolamine could contribute to the 250-fold difference in the  $k_{\text{cat}}$  values of the two substrates.

An interspin distance,  $r$ , of  $8.7 \text{ \AA}$  is obtained using the point-dipole approximation in eq 5 (44)

$$D = -3\mu_0 g^2 \beta^2 / 8\pi r^3 \quad (5)$$

and  $D = -43 \text{ G}$  derived from the spectral simulations. This result places the spin-bearing carbon  $\sim 2.3 \text{ \AA}$  closer to the  $\text{Co}^{2+}$  of cob(II)alamin compared to the distance of  $\sim 11 \text{ \AA}$  in the corresponding substrate radical of (*S*)-2-aminopropanol (29). The structural results obtained from

Scheme 2



the spin–spin interaction parameters are summarized in Scheme 2.

## ACKNOWLEDGMENT

We thank Dr. Steven O. Mansoorabadi for help with computations, Dr. Mark Anderson for acquiring the  $^{13}\text{C}$  NMR spectra, and Drs. Perry Frey and W. W. Cleland for helpful discussion.

## SUPPORTING INFORMATION AVAILABLE

$^{13}\text{C}$  NMR spectra of ( $^{13}\text{C}$ )ethanolamines and  $^1\text{H}$  NMR spectra of ( $^{13}\text{C}$ )glycine precursors and a stopped flow spectrophotometric assay for Co–carbon bond cleavage in the steady state with ethanolamine. This material is available free of charge via the Internet at <http://pubs.acs.org>.

## REFERENCES

- Wallis, O. C., Johnson, A. W., and Lappert, M. F. (1979) Studies on the subunit structure of the adenosylcobalamin-dependent enzyme ethanolamine ammonia-lyase. *FEBS Lett.* 97, 196–199.
- Faust, L. P., and Babor, B. M. (1992) Overexpression, purification, and some properties of the AdoCbl-dependent ethanolamine ammonia-lyase from *Salmonella typhimurium*. *Arch. Biochem. Biophys.* 294, 50–54.
- Roof, D. M., and Roth, J. R. (1988) Ethanolamine utilization in *Salmonella typhimurium*. *J. Bacteriol.* 170, 3855–3863.
- Bandarian, V., and Reed, G. H. (1999) Hydrazine cation radical in the active site of ethanolamine ammonia-lyase: Mechanism-based inactivation by hydroxyethylhydrazine. *Biochemistry* 38, 12394–12402.
- Babor, B. M. (1970) The mechanism of action of ethanolamine deaminase. VI. Ethylene glycol, a quasi-substrate for ethanolamine deaminase. *J. Biol. Chem.* 245, 1755–1766.
- Bandarian, V., and Reed, G. H. (2000) Isotope effects in the transient phases of the reaction catalyzed by ethanolamine ammonia-lyase: Determination of the number of exchangeable hydrogens in the enzyme-cofactor complex. *Biochemistry* 39, 12069–12075.
- Graves, S. W., and Babor, B. M. (1982) Interaction of N-substituted ethanolamine analogs with ethanolamine ammonia-lyase, an adenosylcobalamin-requiring enzyme. *J. Biol. Chem.* 257, 4102–4105.
- Krouwer, J. S., Schultz, R. M., and Babor, B. M. (1978) The mechanism of action of ethanolamine ammonia-lyase, an adenosylcobalamin-dependent enzyme. Reaction of the enzyme-cofactor complex with 2-aminoacetaldehyde. *J. Biol. Chem.* 253, 1041–1047.

9. Wang, M., and Warncke, K. (2008) Kinetic and thermodynamic characterization of Co(II)-substrate radical pair formation in coenzyme B12-dependent ethanolamine ammonia-lyase in a cryo-solvent system by using time-resolved, full-spectrum continuous-wave electron paramagnetic resonance spectroscopy. *J. Am. Chem. Soc.* 130, 4846–4858.
10. Bandarian, V., and Reed, G. H. (1999) Ethanolamine Ammonia-Lyase. In *Chemistry and Biochemistry of B12* (Banerjee, R., Ed.) pp 811–834, Wiley-Interscience, New York.
11. Yan, S.-J., McKinnie, B. G., Abacherli, C., Hill, R. K., and Babior, B. M. (1984) Stereochemistry of the ethanolamine ammonia lyase reaction with stereospecifically labeled [1-<sup>3</sup>H]-2-aminoethanol. *J. Am. Chem. Soc.* 106, 2961–2964.
12. Semialjac, M., and Schwarz, H. (2002) Computational exploration of rearrangements related to the vitamin B12-dependent ethanolamine ammonia lyase catalyzed transformation. *J. Am. Chem. Soc.* 124, 8974–8983.
13. Warncke, K., and Canfield, J. M. (2004) Direct determination of product radical structure reveals the radical rearrangement pathway in a coenzyme B12-dependent enzyme. *J. Am. Chem. Soc.* 126, 5930–5931.
14. Wetmore, S. D., Smith, D. M., Bennett, J. T., and Radom, L. (2002) Understanding the mechanism of action of B12-dependent ethanolamine ammonia-lyase: Synergistic interactions at play. *J. Am. Chem. Soc.* 124, 14054–14065.
15. Babior, B., and Gould, D. C. (1969) An EPR signal generated by the ethanolamine deaminase-coenzyme B12 complex in the presence of substrate. *Biochem. Biophys. Res. Commun.* 34, 441–447.
16. Babior, B. M., Moss, T. H., and Gould, D. C. (1972) The mechanism of action of ethanolamine ammonia lyase, a B12-dependent enzyme. X. A study of the reaction by electron spin resonance spectrometry. *J. Biol. Chem.* 247, 4389–4392.
17. Babior, B. M., Moss, T. H., Orme-Johnson, W. H., and Beinert, H. (1974) The mechanism of action of ethanolamine ammonia-lyase, a B-12-dependent enzyme. The participation of paramagnetic species in the catalytic deamination of 2-aminopropanol. *J. Biol. Chem.* 249, 4537–4544.
18. Poyner, R. R., Anderson, M. A., Bandarian, V., Cleland, W. W., and Reed, G. H. (2006) Probing nitrogen-sensitive steps in the free-radical-mediated deamination of amino alcohols by ethanolamine ammonia-lyase. *J. Am. Chem. Soc.* 128, 7120–7121.
19. Gerfen, G. J. (1999) EPR Spectroscopy of B12-Dependent Enzymes. In *Chemistry and Biochemistry of B12* (Banerjee, R., Ed.) pp 165–195, Wiley-Interscience, New York.
20. Warncke, K., Schmidt, J. C., and Ke, S. C. (1999) Identification of a rearranged-substrate, product radical intermediate and the contribution of a product radical trap in vitamin B-12 coenzyme-dependent ethanolamine deaminase catalysis. *J. Am. Chem. Soc.* 121, 10522–10528.
21. Ke, S. C. (2003) Spin-spin interaction in ethanolamine deaminase. *Biochim. Biophys. Acta* 1620, 267–272.
22. Sheu, M. J., and Ke, S. C. (2005) Molecular properties of the product radical in adenosylcobalamin-dependent ethanolamine deaminase. *Phys. A (Amsterdam, Neth.)* 350, 131–143.
23. Warncke, K. (2005) Characterization of the product radical structure in the Co(II)-product radical pair state of coenzyme B12-dependent ethanolamine deaminase by using three-pulse <sup>2</sup>H ESEEM spectroscopy. *Biochemistry* 44, 3184–3193.
24. Canfield, J. M., and Warncke, K. (2005) Active site reactant center geometry in the Co(II)-product radical pair state of coenzyme B12-dependent ethanolamine deaminase determined by using orientation-selection electron spin-echo envelope modulation spectroscopy. *J. Phys. Chem. B* 109, 3053–3064.
25. Hollaway, M. R., White, H. A., Joblin, K. N., Johnson, A. W., Lappert, M. F., and Wallis, O. C. (1978) A spectrophotometric rapid kinetic study of reactions catalysed by coenzyme B12-dependent ethanolamine ammonia-lyase. *Eur. J. Biochem.* 82, 143–154.
26. Jones, A. R., Hay, S., Woodward, J. R., and Scrutton, N. S. (2007) Magnetic field effect studies indicate reduced geminate recombination of the radical pair in substrate-bound adenosylcobalamin-dependent ethanolamine ammonia-lyase. *J. Am. Chem. Soc.* 129, 15718–15727.
27. Kaplan, B. H., and Stadtman, E. R. (1968) Ethanolamine deaminase. A cobamide coenzyme-dependent enzyme. *J. Biol. Chem.* 243, 1787–1793.
28. Beinert, H., Hansen, R. E., and Hartzell, C. R. (1976) Kinetic studies on cytochrome c oxidase by combined epr and reflectance spectroscopy after rapid freezing. *Biochim. Biophys. Acta* 423, 339–355.
29. Bandarian, V., and Reed, G. H. (2002) Analysis of the electron paramagnetic resonance spectrum of a radical intermediate in the coenzyme B(12)-dependent ethanolamine ammonia-lyase catalyzed reaction of (S)-2-aminopropanol. *Biochemistry* 41, 8580–8588.
30. Goldstein, H., Poole, C., and Safko, J. L. (2002) *Classical Mechanics*, 3rd ed., pp 150–154, Addison-Wesley, San Francisco.
31. Mansoorabadi, S. O., Padmakumar, R., Fazliddinova, N., Vlasie, M., Banerjee, R., and Reed, G. H. (2005) Characterization of a succinyl-CoA radical-cob(II)alamin spin triplet intermediate in the reaction catalyzed by adenosylcobalamin-dependent methylmalonyl-CoA mutase. *Biochemistry* 44, 3153–3158.
32. Abend, A., Bandarian, V., Nitsche, R., Stupperich, E., Retey, J., and Reed, G. H. (1999) Ethanolamine ammonia-lyase has a “base-on” binding mode for coenzyme B12. *Arch. Biochem. Biophys.* 370, 131–141.
33. Ke, S.-C., Torrent, M., Museav, D. G., Morokuma, K., and Warncke, K. (1999) Identification of dimethylbenzimidazole axial coordination and characterization of <sup>14</sup>N superhyperfine and nuclear quadrupole coupling on Cob(II)alamin bound to ethanolamine deaminase in a catalytically-engaged substrate radical-cobalt(II) biradical state. *Biochemistry* 38, 12681–12689.
34. Bender, G. (2008) Ph.D. Dissertation, pp 135, University of Wisconsin, Madison, WI.
35. Bencini, A., and Gatteschi, D. (1990) Exchange and Superexchange. In *EPR of Exchange Coupled Systems*, pp 1–19, Springer-Verlag, Berlin.
36. Mansoorabadi, S. O., and Reed, G. H. (2003) Effects of electron spin delocalization on non-colinearity of interaction terms in EPR triplet powder patterns. In *Paramagnetic Resonance of Metallobiomolecules* (Telser, J., Ed.) pp 82–96, American Chemical Society, Washington, DC.
37. Sun, L., Groover, O. A., Canfield, J. M., and Warncke, K. (2008) Critical role of arginine 160 of the EutB protein subunit for active site structure and radical catalysis in coenzyme B12-dependent ethanolamine ammonia-lyase. *Biochemistry* 47, 5523–5535.
38. Warncke, K., Schmidt, J. C., and Ke, S.-C. (2008) Identification of a rearranged-substrate, product radical intermediate and the contribution of a product radical trap in vitamin B12 coenzyme-dependent ethanolamine deaminase catalysis. *J. Am. Chem. Soc.* 130, 6055.
39. Wertz, J. E., and Bolton, J. R. (1986) *Electron Spin Resonance*, pp 170–171, Chapman and Hall, New York.
40. Gordy, W. (1980) *Theory and Applications of Electron Spin Resonance*, pp 244–247, Wiley, New York.
41. Frey, P. A. (2001) Radical mechanisms of enzymatic catalysis. *Annu. Rev. Biochem.* 70, 121–148.
42. Frey, P. A., and Hegeman, A. D. (2007) *Enzymatic Reaction Mechanisms*, pp 97–99, Oxford University Press, Oxford, U.K.
43. Cook, P. F., and Cleland, W. W. (2007) *Enzyme Kinetics and Mechanism*, pp 253–295, Garland Science, New York.
44. Luckhurst, G. R. (1976) Biradicals as spin probes. In *Spin Labeling: Theory and Applications* (Berliner, L. J., Ed.) pp 133–181, Academic Press, New York.

BI801316V